EBioMedicine 47 (2019) 553–562

Contents lists available at ScienceDirect

EBioMedicine

journal homepage: www.ebiomedicine.com

EBioMedicine
Published by THE LANCET

Research paper

Transplantation studies reveal internuclear transfer of toxic RNA in engrafted muscles of myotonic dystrophy 1 mice

Ricardo Mondragon-Gonzalez [a,b], Karim Azzag [a,1], Sridhar Selvaraj [a,1], Ami Yamamoto [a], Rita C.R. Perlingeiro [a,c,*]

[a] Lillehei Heart Institute, Department of Medicine, University of Minnesota, Minneapolis, MN, USA
[b] Departamento de Genética y Biología Molecular, Centro de Investigación y de Estudios Avanzados del IPN (CINVESTAV-IPN), Mexico City, Mexico
[c] Stem Cell Institute, University of Minnesota, Minneapolis, MN, USA

ARTICLE INFO

Article history:
Received 9 February 2019
Received in revised form 5 August 2019
Accepted 14 August 2019
Available online 21 August 2019

Keywords:
Autosomal dominant
Myotonic dystrophy 1
Induced pluripotent stem (iPS) cells
Cell therapy
HSA^{LR}
Muscular dystrophy
PAX7
RNA foci
Human-specific splicing

ABSTRACT

Background: Stem cell transplantation represents a potential therapeutic option for muscular dystrophies (MD). However, to date, most reports have utilized mouse models for recessive types of MD. Here we performed studies to determine whether myotonic dystrophy 1 (DM1), an autosomal dominant type of MD, could benefit from cell transplantation.
Methods: We injected human pluripotent stem (PS) cell-derived myogenic progenitors into the muscles of a novel mouse model combining immunodeficiency and skeletal muscle pathology of DM1 and investigated transplanted mice for engraftment as well as for the presence of RNA foci and alternative splicing pattern.
Findings: Engraftment was clearly observed in recipient mice, but unexpectedly, we detected RNA foci in donor-derived engrafted myonuclei. These foci proved to be pathogenic as we observed MBNL1 sequestration and abnormal alternative splicing in donor-derived transcripts.
Interpretation: It has been assumed that toxic CUG repeat-containing RNA forms foci *in situ* in the nucleus in which it is expressed, but these data suggest that CUG repeat-containing RNA may also exit the nucleus and traffic to other nuclei in the syncytial myofiber, where it can exert pathological effects.
Fund: This project was supported by funds from the LaBonte/Shawn family and NIH grants R01 AR055299 and AR071439 (R.C.R.P.). R.M-G. was funded by CONACyT-Mexico (#394378).

1. Introduction

Myotonic Dystrophy 1 (DM1) is an autosomal dominant multisystemic disorder with an estimated prevalence of 1/10,000 worldwide, although this varies among populations [1,2]. Several tissues are affected in DM1, and in particular skeletal muscle undergoes progressive weakness and wasting, along with myotonia [3,4]. DM1 is caused by an expansion of the CTG triplet repeats contained in the 3'UTR of the dystrophia myotonica protein kinase *(DMPK)* gene [5]. *DMPK* transcripts containing expanded CUG triplets fold into extended stem-loop structures that accumulate as intranuclear RNA foci [6–9]. Most of the clinical manifestations of DM1 have been related to the sequestration of the alternative splicing factor muscleblind-like protein 1 (MBNL1) by the RNA foci, which alters the proper alternative splicing of MBNL1 target genes [10–12].

Several mouse models have been developed to study DM1 pathology [13–15]. Among these, the HSA^{LR} mouse model [14], which expresses 250 CUG repeats in the context of the human skeletal actin gene, has been widely used to study DM1 skeletal muscle phenotype and potential treatment strategies aiming to recover the mis-splicing alterations. Despite progress, clinical trials tested so far, such as the use of modified antisense oligonucleotides to eliminate toxic RNA foci [16–18], have failed to provide significant improvement in DM1 patients mainly due to limited drug uptake in muscle (ClinicalTrials.gov, NTC02312011). Thus, therapeutic strategies that ameliorate the muscle disease phenotype in DM1 are warranted.

Cell-based therapy has emerged as a promising treatment strategy for recessive muscular dystrophies [19–21]. For instance, it has been shown that transplantation of myogenic precursors in mouse models of Duchenne muscular dystrophy (DMD) leads to the generation of donor-derived new myofibers and hybrid myofibers containing donor-derived myonuclei, which are able to provide dystrophin, thus resulting in functional improvement [22–26]. However, the feasibility of cell-based therapy for dominant MDs is complicated by the fact that the muscle fiber is a syncytium. This means that if mutant nuclei are

* Corresponding author at: Lillehei Heart Institute, University of Minnesota, 4-128 CCRB, 2231 6th St. SE, Minneapolis, MN 55455, USA.
E-mail address: perli032@umn.edu (R.C.R. Perlingeiro).
[1] Contributed equally

https://doi.org/10.1016/j.ebiom.2019.08.031

Research in context

Evidence before this study

We and others have previously demonstrated the beneficial outcome of cell transplantation in mouse models of recessive types of muscular dystrophies. In this context, donor-derived engrafted myonuclei are able to provide fully functional proteins that overcome the phenotype of absent or mutated endogenous proteins, such as dystrophin in the case of Duchenne muscular dystrophy (DMD). However, to date, limited literature exists in the context of cell transplantation for dominant types of muscular dystrophies, and none for myotonic dystrophy 1 (DM1).

Added value of this study

Here we assessed for the first time whether DM1 could be a potential candidate for cell-based therapy. Unexpectedly, our findings revealed that toxic RNAs produced in the endogenous nuclei of DM1 recipient mice are transmitted to donor-derived nuclei, leading to alterations in the alternative splicing of donor-derived transcripts.

Implications of all the available evidence

Our findings suggest a pathomechanism for DM1, in which toxic RNAs are able to exit the nucleus in which they were synthesized to exert pathological effects in other myonuclei within the syncytium. Although expression of toxic RNA in the DM1 mouse model is different from DM1 patients, one cannot exclude the possibility of foci acquisition by normal cells in the scenario DM1 patients receive cell transplantation. This is also relevant for alternative strategies, such as gene editing, as non-corrected myonuclei producing toxic RNAs may affect the alternative splicing of successfully gene-corrected myonuclei within the syncytium.

not completely eliminated, there will always be some background expression of the dominant disease-causing gene.

To address this question, here we performed transplantation studies using a novel immunodeficient DM1 mouse model. Successful engraftment was achieved, but unexpectedly, we observed the presence of pathogenic RNA foci in donor-derived nuclei of hybrid myofibers. These results shed light on a novel dynamic behavior of toxic RNA foci among myonuclei, with potential implications for the efficacy of cell therapy for DM1.

2. Materials and methods

2.1. Mice

Animal handling was performed according to protocols approved by the University of Minnesota Institutional Animal Care and Use Committee. Breeding pairs of homozygous HSA^{LR} mice [14] were kindly provided by Dr. Charles Thornton (University of Rochester, NY). NSG [27,28] and CAG:H2B-EGFP [29] mice were purchased from Jackson Laboratories (005557 and 006069, respectively). HSA^{LR} were bred to NSG mice to obtain a homozygous $HSA^{LR\,(+/+)}\,NS^{(+/+)}G^{(+)}$ colony. HSA^{LR} transgene homozygosity and CTG length confirmation were carried out as previously described [30].

2.2. Peripheral blood FACS analysis

Peripheral blood from facial vein of HSA^{LR}, NSG and NSG-HSA^{LR} mice was collected onto EDTA-containing tubes. Samples were sequentially incubated with RBC lysis buffer (Biolegend) for 5 min at room temperature (RT), and FcR blocking antibody for 5 min on ice. Then, cells were resuspended in FACS buffer (10% FBS in PBS) and incubated with appropriate antibodies for 20 min on ice. Antibodies are listed in Table S1. FACS analysis was performed using a FACSAria (BD Biosciences). Data were analyzed using FlowJo software.

2.3. Cell transplantation

For transplantation studies, we used myogenic progenitors derived from the previously reported human iPAX7 PLZ iPS cell line [26,31]. Mouse myogenic progenitors were generated from inducible Pax3 (iPax3) mES cells, as previously described [32–34]. Mouse satellite cells were isolated from several muscles, as reported [35]. For the transplantation of mES cell-derived myogenic progenitors into HSA^{LR} mice, these mice received daily intra-peritoneal (IP) injections of the immunosuppressant agent Tacrolimus (AKSci) at a dose of 5 mg/kg. Treatment began two days before transplantation and ended by the day of euthanasia [36]. mES cell-derived myogenic progenitors, hiPS cell-derived myogenic progenitors and human skeletal myoblasts (HSKM) (Gibco) were injected at $7{\cdot}5 \times 10^5$ cells, and H2B-eGFP satellite cells at 5×10^3 cells. Cells resuspended in 15 μl of PBS were injected into the TA muscles that had been pre-injured 24 h prior to cell transplantation with either 15 μl of 10 μM cardiotoxin, 15 μl of 1·2% barium chloride in saline solution, or by freeze injury [26,37]. Freeze injury was performed by applying a liquid nitrogen-cooled spatula directly on the exposed muscle twice for 10 s with a 1 min interval in-between [38]. TA muscles were dissected four weeks after transplantation and resulting cryosections (10 μm) were evaluated, as described below.

2.4. RNA-FISH/DNA-FISH/immunofluorescence

To identify nuclei containing human DNA, we performed DNA FISH using human Cot-1 as a probe [39,40]. Cot human DNA (Roche) was labelled using the Atto647N NT labeling kit (Jena Bioscience) following the manufacturer's instructions. Labelled probe was then purified using QIAquick PCR purification kit (QIAGEN). DNA FISH protocol was performed as follows: muscle cryosections on glass slides were thawed to RT and hydrated with PBS for 5 min. Then, sections were fixed with 4% PFA for 30 min, permeabilized with 0·3% Triton X-100 for 15 min, rinsed with 2× SSC and then incubated with denaturation buffer (70% formamide in 2× SSC) for 10 min at 80 °C in a humid chamber. Samples were then incubated with probe solution (2× SSC, 50% formamide, 2 mM ribonucleoside vanadyl complex, 75 ng/μl tRNA and 4 ng/μl of labelled probe) for 7 min at 80 °C, followed by overnight incubation at 37 °C. Probe solution was heated for 10 min at 80 °C prior to incubation. The next day, slides were washed with 50% formamide in 2× SSC for 5 min at 41 °C and then washed again with 2× SSC at RT. Slides were then processed for RNA FISH-immunofluorescence starting with the pre-hybridization buffer incubation step (see RNA FISH protocol below).

To detect the intranuclear RNA foci, muscle cryosections were fixed with 4% PFA for 10 min, permeabilized with 0·3% Triton X-100 for 15 min, and incubated with pre-hybridization buffer solution (2 x SSC and 30% formamide in DEPC water) for 10 min at RT. Samples were incubated with hybridization solution (2× SSC, 30% formamide, 0·02% BSA, 2 mM ribonucleoside vanadyl complex, 66 μg/ml yeast tRNA and 0.1 ng/ul of a Cy3-labelled $(CAG)_7$ probe in DEPC water) for 2 h at 37 °C in a humid chamber. Samples were washed twice with pre-hybridization buffer solution for 7 min at 42 °C and two more times with 1× SSC in DEPC water for 5 min at RT. Samples were then processed for immunostaining: first slides were blocked with 3% BSA in PBS for 30 min, followed by incubation overnight with selected primary antibodies at 4 °C. The following day, samples were washed three times with PBS for 5 min and incubated with proper secondary antibodies for 1 h at RT. Samples were washed again 3× with PBS for 5 min and

mounted with ProLong Gold antifade reagent with DAPI (Invitrogen). Analysis was done by confocal microscopy (Nikon NiE C2 upright confocal microscope). Antibodies are listed in Table S1.

2.5. RT-PCR

Samples were collected with TRIzol™ Reagent (Invitrogen) and RNA was purified using the Direct-zol™ RNA Miniprep Plus kit (Zymo Research) following manufacturer's instructions. Purified RNA was quantified with NanoDrop 2000 (Thermo Scientific) and reverse-transcribed using the SuperScript VILO cDNA Synthesis Kit (Invitrogen) following manufacturer's instructions. cDNA was used as template for PCR using GoTaq Flexi DNA polymerase (Promega). Primers that have been previously reported were used to analyze *Clcn1* exon 7A [41], *Nfix* exon 7 [41], *Serca1* exon 22 [42], *Gapdh* [41], human specific *SERCA1 exon 22* [43] and human specific *LDB3* exon 11 [44]. Primers for *ACTB*: Fwd 5' CATGTACGTTGCTATCCAGGC 3′ and Rev. 5' CTCCTTAATGTCACGCACG AT 3′; and human specific *CACNA1S* exon 29: Fwd 5' CTGATTGTCAT TGGCAGCAT 3′ and Rev. 5' AGGGTTCGCACTCCTTCTG 3′.

2.6. Statistical analysis

Statistical comparisons were performed using the unpaired Student's *t*-test in Prism 7 software (GraphPad). *p* values <0·05 were considered significant.

3. Results

3.1. Generation of an immunodeficient mouse model for DM1

To provide an ideal environment for the transplantation of mouse and human cells, we have crossed the HSA^{LR} mutant DM1 strain [14] onto the NSG (NOD/SCID; IL2 receptor gamma) background [28]. NSG mice lack all functional classes of lymphocytes (T, B, and NK cells) [45,46], and therefore are widely used for xenotransplantation studies [24,28,47]. Upon obtaining NSG-HSA^{LR} homozygous at all loci, the peripheral blood of these mice was characterized for the lack of T, B and NK cells, whereas the skeletal muscle was tested for the presence of RNA foci. FACS analysis confirmed the absence of NK cells (NK 1.1^{+}CD49b^{+} cells), as well as T and B lymphocytes (CD3e^{+} and CD19^{+} cells, respectively) in NSG-HSA^{LR} mice, in contrast to immunocompetent HSA^{LR} mice (Fig. 1a), which contained all these lymphocyte subtypes.

To verify the presence of typical DM1 molecular hallmarks, we performed RNA FISH, using a labelled probe that detects the expanded CUG repeats, combined with immunostaining for MBNL1. Similar to homozygous HSA^{LR} mice (Fig. S1), NSG-HSA^{LR} mice displayed intranuclear RNA foci that co-localized with MBNL1 labelling, confirming the sequestration of MBNL1 by the mutant RNA aggregates (Fig. 1b). As anticipated, these features were not found in control non-DM1 immunodeficient mice (Fig. S1). Furthermore, we also confirmed significant alterations in alternative splicing of MBNL1 target genes, including *Clcn1* exon 7A inclusion, *Nfix* exon 7 inclusion and *Serca1* exon 22 exclusion (Fig. 1c-d). These results validate this novel mouse model as NSG-HSA^{LR} mice combine the immunodeficiency features of NSG mice with the DM1 molecular features of HSA^{LR} mice.

3.2. Engraftment of iPS cell-derived myogenic progenitors in NSG-HSA^{LR} mice

To determine whether cell transplantation could be used to overcome the splicing defects observed in DM1, we injected human iPS cell-derived myogenic progenitors [26] into cardiotoxin pre-injured TA muscles of NSG-HSA^{LR} mice. A cohort of NSG mice was used as control recipients. Four weeks post-transplantation, we assessed human engraftment by performing immunostaining of muscle cryosections with antibodies specific to human Lamin A/C (hLMNA/C) and human Dystrophin (hDYS). We detected donor-derived myofibers (hLMNA/C + hDYS+) in both NSG-HSA^{LR} and NSG mice (Fig. 2a), and at similar levels (Fig. 2b), corroborating the usefulness of the NSG-HSA^{LR} mouse model for the transplantation of human cells. Importantly, no labelling signal was detected in TA muscles that had been injected with PBS (control), thus confirming the human specificity of used antibodies (Fig. S2).

3.3. Identification of RNA foci in donor-derived myonuclei

To determine whether engraftment reduced the presence of toxic foci, we performed RNA-FISH on muscle sections of transplanted NSG-HSA^{LR} mice. To our surprise, we detected the foci not only in the endogenous host mouse nuclei, but also in human donor-derived myonuclei (hLMNA/C+ nuclei within hDYS+ myofibers) (Fig. 3a, upper panel). This result was specific to NSG-HSA^{LR} mice since no such foci could be detected in control NSG recipients transplanted with the same cell population (Fig. 3a, lower panel).

We reasoned that the presence of foci in donor-derived nuclei could be a result of fusion of non-affected human myogenic progenitors with pre-existing DM1 mouse muscle fibers, in which human Lamin A/C proteins would be synthesized and directed to mouse nuclei within the fiber, thereby falsely identifying host nuclei as donor-derived. To rule out this hypothesis, we performed immunostaining to hLMNA/C in combination with DNA FISH using human Cot-1 as a probe to specifically label nuclei containing human DNA (hDNA) [40]. Importantly, no hDNA signal was observed in PBS-injected muscles (Fig. S2), thus confirming the reliability of the combined methodologies to identify cells of human origin. Lastly, we incorporated RNA-FISH to assess the number of human myonuclei containing foci. We observed that from the total of hLMNA/C+ myonuclei, 67% were also positive for hDNA. From these double positive myonuclei, 65% were also positive for RNA foci (Fig. 3b-c) (Statistical analysis is shown in Table S2). Of note, within the same fiber, we detected the presence of mouse nuclei, absent of hDNA or hLMNA/C labelling, but positive for RNA foci (Fig. 3b). These results indicate that non-affected human myogenic nuclei acquired intranuclear RNA foci, likely through the shared cytoplasm of a chimeric fiber. In accordance, RNA foci transfer was also observed upon the transplantation of mouse embryonic stem (mES) cell-derived myogenic progenitors [32,33] into tacrolimus-treated immunocompetent HSA^{LR} mice, as shown by the presence of foci in donor-derived H2B-GFP+ nuclei (nGFP) (Fig. S3, upper panel).

To determine whether RNA foci transfer was related in some way to cardiotoxin, we performed cell transplantation in the context of other types of muscle injury, including freezing injury and $BaCl_2$ injection. The same outcome was obtained, regardless of the pre-injury method used (Fig. S4A).

Interestingly, when we performed a reverse experiment, in which patient-specific DM1 myogenic progenitors [48] or HSA^{LR} satellite cells were transplanted into TA muscles of control NSG mice, we did not detect RNA foci in host myonuclei (data not shown). These results may be due to the low abundance of engrafted myonuclei providing mutant transcripts in comparison with host myonuclei within the myofiber of HSA^{LR} mice.

3.4. RNA foci present in donor-derived human myonuclei are pathogenic

To understand the biological relevance of RNA foci detected in engrafted human myonuclei, we first analyzed MBNL1 distribution and observed its sequestration by the acquired foci (Fig. 4a), thus suggesting a toxic effect. Next we determined whether MBNL1 sequestration would have subsequent consequences in the alternative splicing pattern of human *SERCA1* exon 22, *LDB3* exon 11 and *CACNA1S* exon 29, which have been shown to be altered in DM1 [11,44,49]. RT-PCR analysis was performed using primers specific to human transcripts, as shown by analysis of control PBS-injected TA muscles as well as

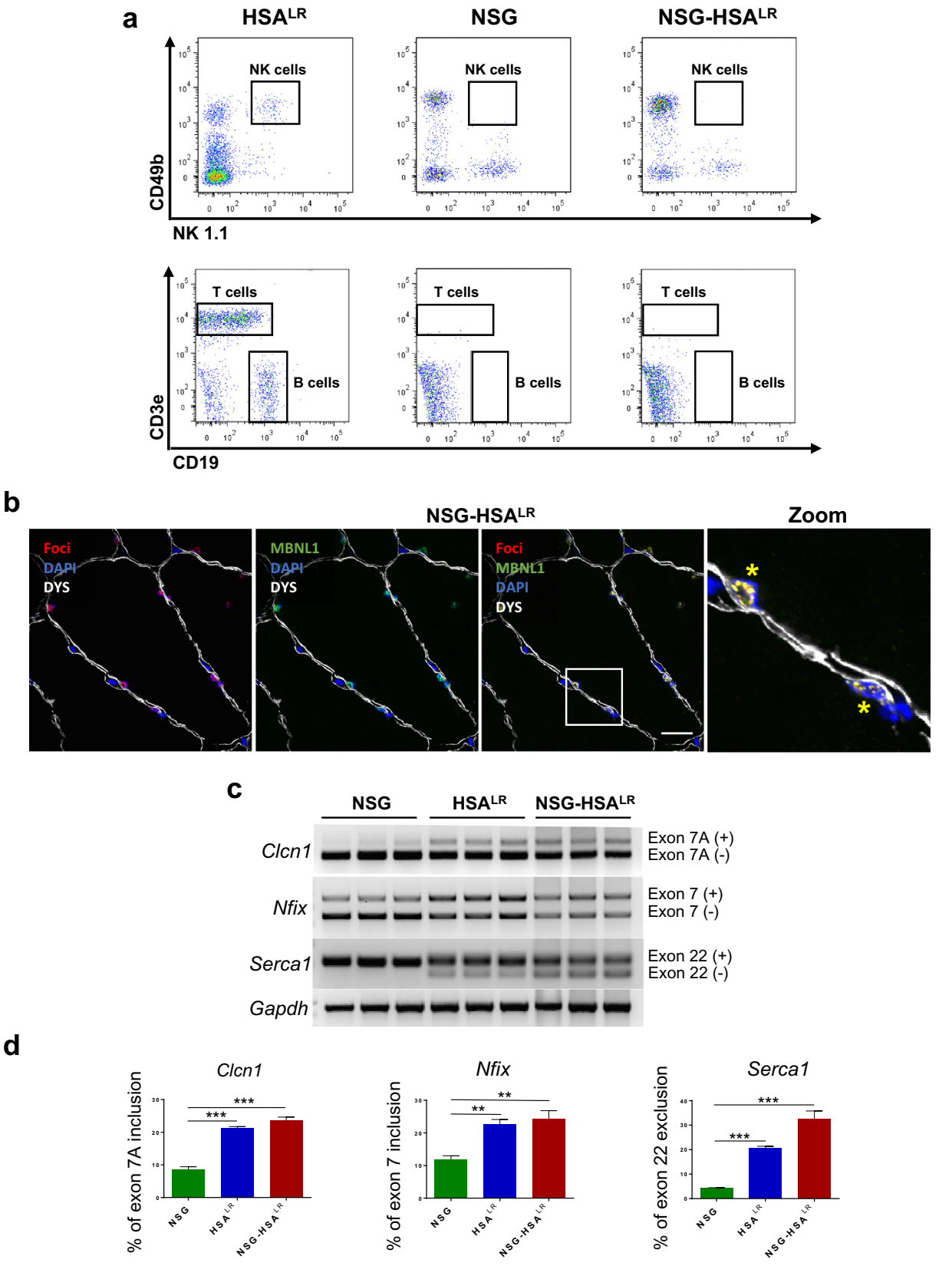

Fig. 1. Characterization of immunodeficiency and DM1 features in NSG-HSA^{LR} mice. (a) FACS profile for circulating NK (CD49b/NK1.1), T (CD3e) and B (CD19) cells in HSA^{LR}, NSG, and NSG-HSA^{LR} mice. (b) Representative images show RNA-FISH analysis (foci, red) in combination with immunostaining for MBNL1 (green) and pan-dystrophin (DYS, white) in muscle sections of NSG-HSA^{LR} mice. DAPI stains nuclei (blue). Asterisks indicate co-localization between foci and MBNL1. Scale bar is 20 μm. Maximum projection is shown. (c) Alternative splicing pattern analysis of *Clcn1* exon 7A, *Nfix* exon 7 and *Serca1* exon 22 in TA muscles from NSG, HSA^{LR} and NSG-HSA^{LR} mice. (d) Bar graphs represent densitometric quantification of *Clcn1* exon 7A inclusion, *Nfix* exon 7 inclusion, or *Serca1* exon 22 exclusion from three independent replicates (from c). Data are shown as mean + SEM. $^{***}p < 0{\cdot}001$. $N = 3$ muscles, one per mouse.

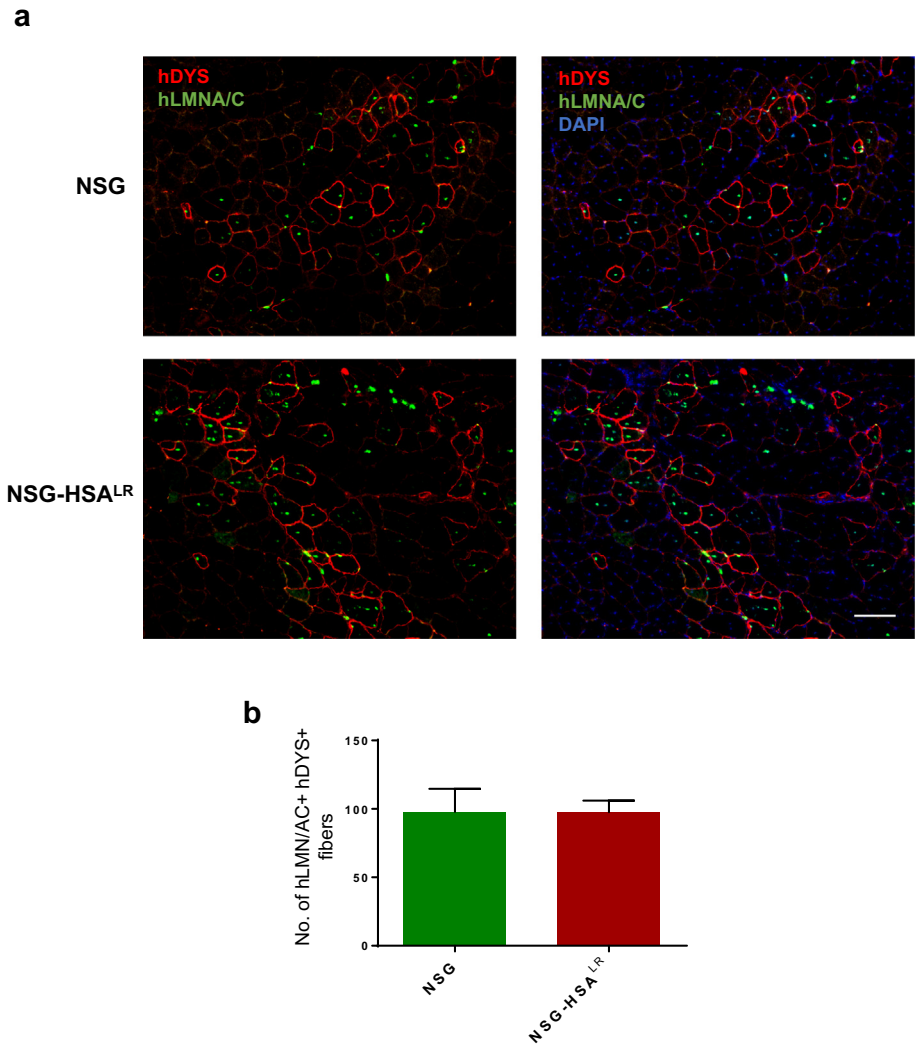

Fig. 2. Engraftment of myogenic progenitors upon their intra-muscular transplantation into NSG-HSA^{LR} mice. (a) Representative images show human engraftment as demonstrated by immunostaining for human DYSTROPHIN (hDYS) and human LAMIN A/C (hLMNA/C) in cryosections of TA muscles from NSG (upper panel) and NSG-HSA^{LR} (lower panel) mice that had been injected with human iPS cell-derived myogenic progenitors. Nuclei (blue). Scale bar is 100 μm. (b) Quantification of engraftment, as shown by the number of double-positive hDYS^{+}/hLMNA/C^{+} myofibers (from a). Data are shown as mean + SEM, $N = 4$ transplanted muscles, one per mouse.

non-injected gastrocnemius muscle (Fig. 4b). While transplantation of non-affected human myogenic progenitors into NSG mice resulted in a splicing pattern similar to non-affected human muscle tissue, transplantation into NSG-HSA^{LR} mice resulted in alterations of alternative splicing in human transcripts, similar to the ones reported in DM1 i. e. exclusion of *SERCA1* exon 22, inclusion of *LDB3* exon 11, and exclusion of *CACNA1S* exon 29 (Fig. 4b and d). To rule out the possibility that this finding was exclusive to the transplanted cell type, we performed similar intramuscular transplantation studies using primary human skeletal myoblasts (HSkM). Again, we observed hLMNA/C^{+} nuclei containing RNA foci in NSG-HSA^{LR}, but not in NSG mice (Fig. S4b), and this was accompanied by alternative splicing alterations of donor-derived transcripts (Fig. 4c-d), thus corroborating our previous observations with PS cell-derived myogenic progenitors.

In another experimental cohort, we isolated satellite cells from CAG: H2B-eGFP mice [29], which allowed us to identify donor-derived nuclei through nuclear GFP labelling (as shown in Fig. S3 for mES-derived myogenic progenitors), and transplanted these into NSG-HSA^{LR} mice. Consistent with previous results, nGFP^{+} nuclei were also found positive for RNA foci (Fig. 5a), and accordingly, no changes in splicing pattern was observed in transplanted muscles (Fig. 5b-c).

4. Discussion

Although several attempts have been made to improve the muscle pathology in DM1, to date, there is no effective treatment available. Therefore, there is still a need to develop novel therapeutic approaches with the potential to improve patient's quality of life. In this regard, cell-based therapy has demonstrated promising results in the recovery of muscle function when applied to recessive muscular dystrophies (*e.g.* DMD), diseases in which donor-derived cells are able to provide a functional molecule when the endogenous one is missing or defective as a consequence of a given genetic condition. This can occur through the generation of new myofibers and/or by fusion with preexistent ones. In an autosomal dominant MD context however, this may be more challenging as engrafted cells need to overcome the molecular hurdles associated with the dominant allele that continuously damage the muscle fiber. In this regard, there has been limited discussion about the importance of disease etiology on cell transplantation efficiency. In DM1, sequestration of MBNL1 by RNA foci leads to alternative splicing alterations in genes that are important to maintain muscle structure and function. If toxic RNAs were retained in their nuclei of origin, one would expect that cell transplantation in DM1 would provide mRNAs

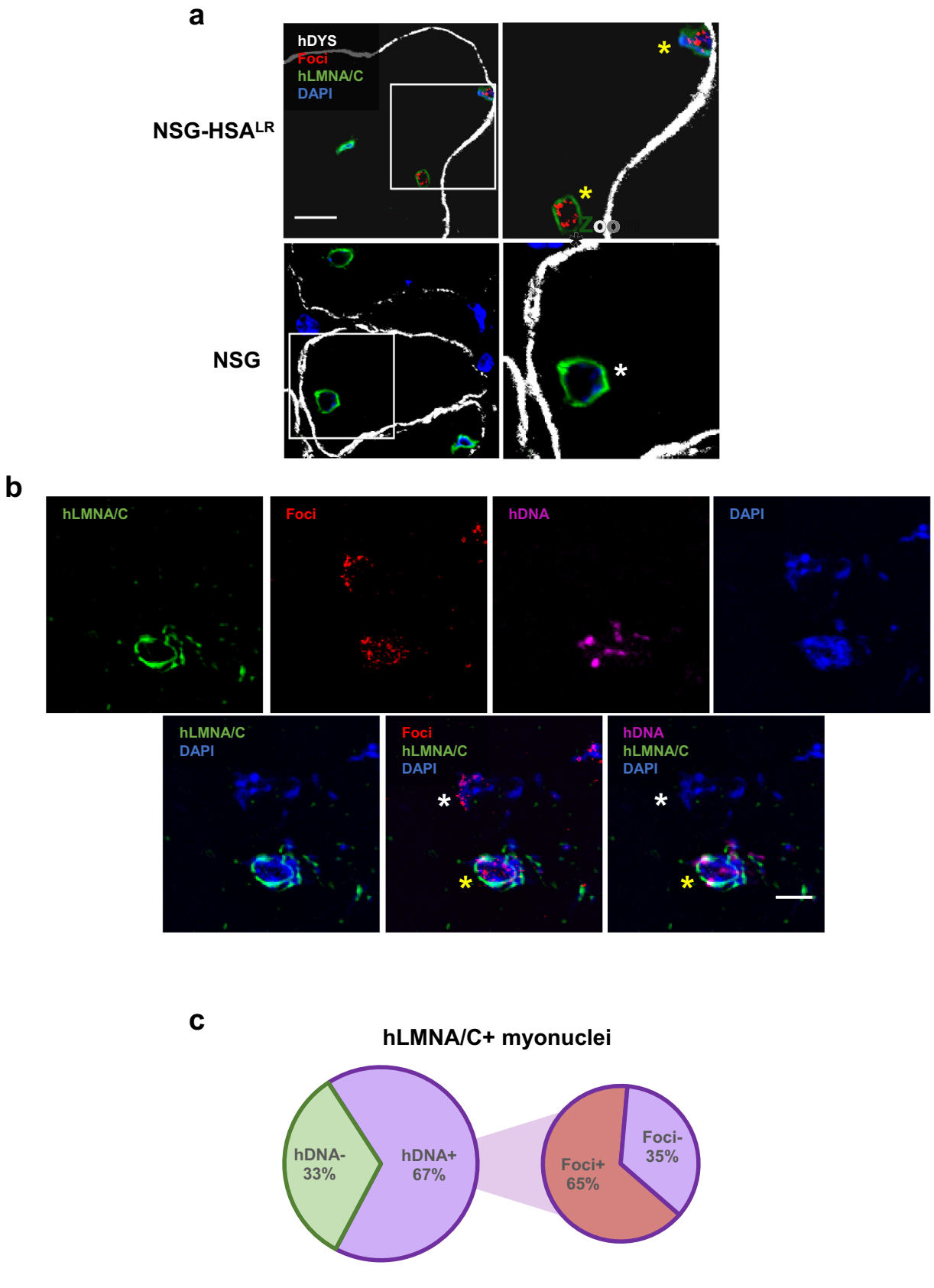

Fig. 3. Detection of toxic RNA foci in donor-derived engrafted myonuclei. (a) Representative images show RNA-FISH analysis (foci in red) in combination with immunostaining for hDYS (white) and hLMNA/C (green) in transplanted TA muscles of NSG-HSA^{LR} (upper panel) and NSG (lower panel) mice. Nuclei (blue). Yellow asterisks in the upper panel indicate human donor-derived myonuclei positive for the foci (NSG-HSA^{LR} recipients), and white asterisk (lower panel) shows human donor-derived myonuclei negative for RNA foci in engrafted NSG mice muscles. Scale bar is 20 μm. Mid Z projection is shown. (b) Representative images confirm the human origin of engrafted hLMNA/C+ myonuclei (green) containing RNA foci (red), as evidenced by detection of human DNA content (hDNA, purple) by DNA-FISH analysis in transplanted NSG-HSA^{LR}. Asterisks show NSG-HSA^{LR} endogenous myonucleus (white) and donor-derived myonucleus (yellow) Scale bar is 5 μm. Mid Z projection is shown. (c) Pie charts show the quantification hLMNA/C+ myonuclei positive for hDNA and RNA foci in TA muscles of NSG-HSA^{LR} mice transplanted with hiPSC-derived myogenic progenitors ($N = 6$ transplanted muscles, one per mouse; 160 total nuclei).

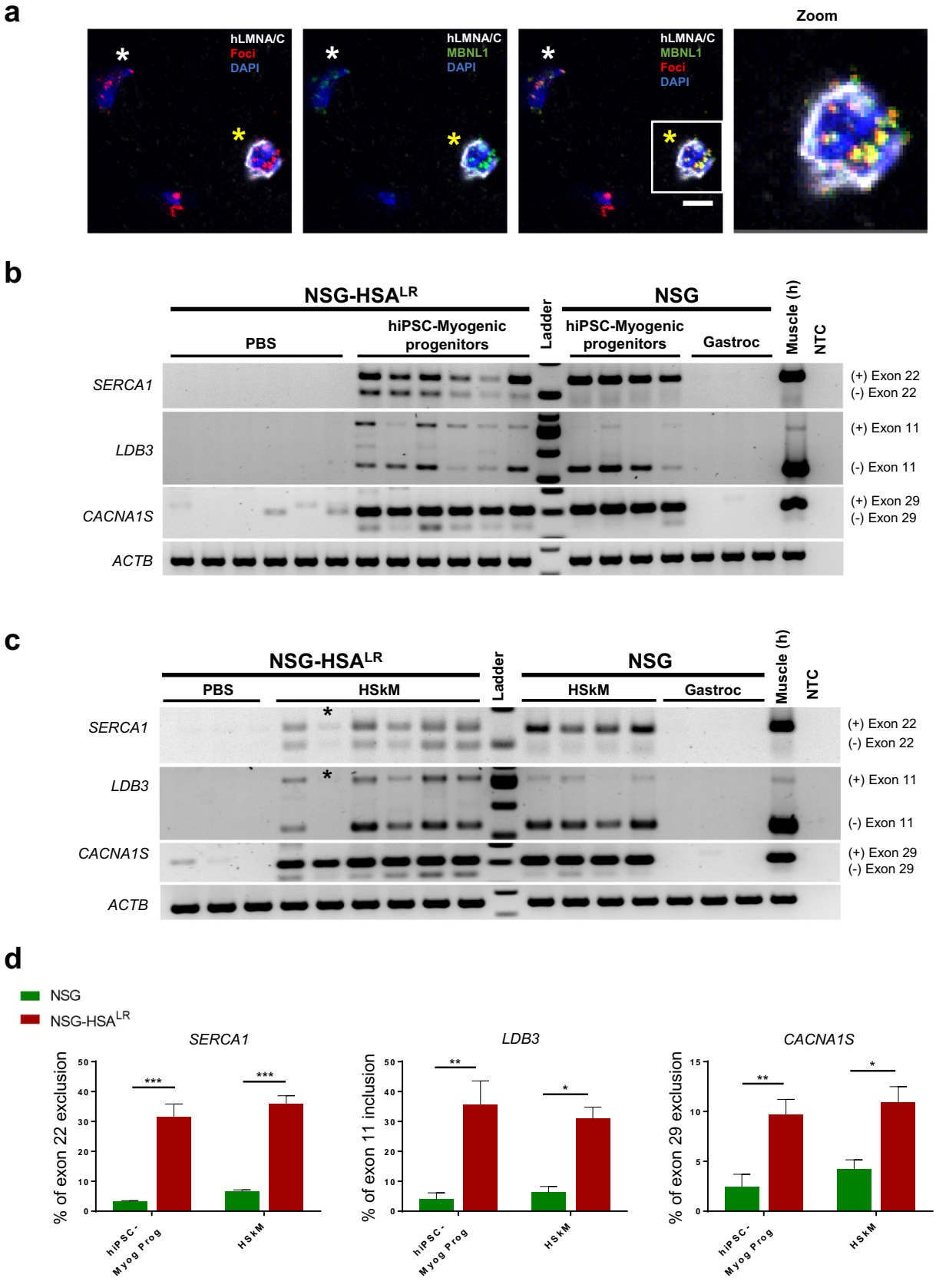

Fig. 4. Pathogenic features of RNA foci detected in donor-derived engrafted myonuclei. (a) Representative images show MBNL1 (green) sequestration by RNA foci (red) in human-derived myonuclei expressing hLMNA/C (white). Asterisks indicate NSG-HSA^{LR} endogenous myonucleus (white) or donor-derived engrafted myonucleus (yellow). Scale bar is 5 μm. Mid Z projection is shown. (b-c) RT-PCR shows alternative splicing analysis of human-specific *SERCA1* exon 22, *LDB3* exon 11 and *CACNA1S* exon 29 in TA muscles from NSG or NSG-HSA^{LR} mice injected with PS cell-derived myogenic progenitors (b) and human skeletal myoblasts (c). Controls included PBS-injected TA muscles, gastrocnemius as a non-injected muscle, and human muscle cDNA as a reference of non-affected alternative splicing. *Samples not quantified due to low amplicon detection. (d) Bar graphs show densitometric analysis of human specific alternative splicing events from (b) and (c) in transplanted muscles of NSG (N = 4 transplanted muscles, one per mouse) and NSG-HSA^{LR} (N = 6 transplanted muscles, one per mouse) mice. Data are shown as mean + SEM. * $p \le 0{\cdot}05$ **$p \le 0{\cdot}01$ ***$p \le 0{\cdot}001$.

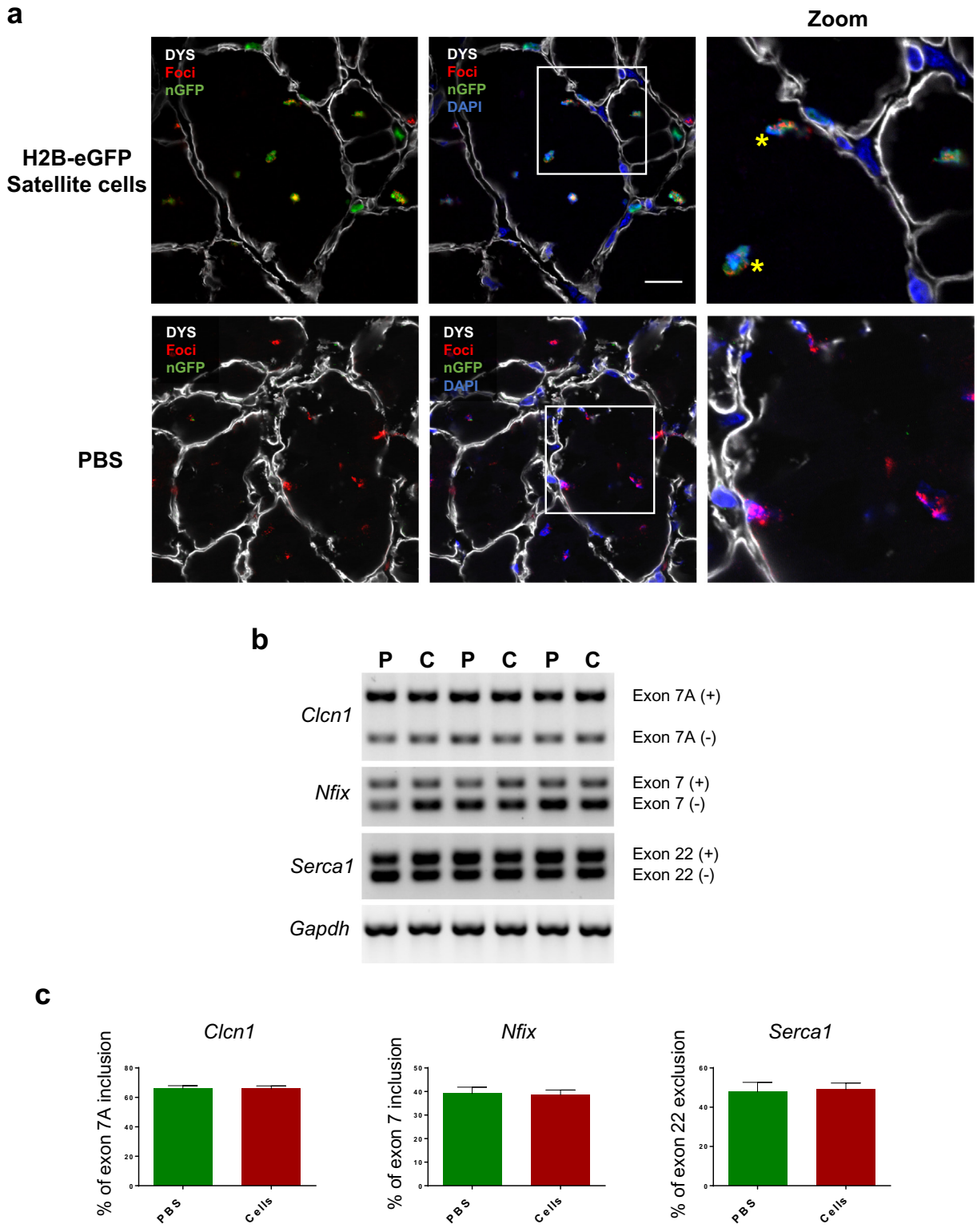

Fig. 5. Detection of toxic RNA foci in donor-derived myonuclei upon satellite stem cell transplantation. (a) Upper panels show representative images for the engraftment of satellite cells isolated from a H2B-eGFP reporter mouse, as shown by the presence of nGFP (green) positive for RNA foci (red). Lower panels show PBS-injected muscles, which are negative for nGFP and positive for the foci. DYS (white) allows myofiber visualization. Asterisks indicate donor-derived engrafted myonuclei. Scale bar is 20 μm. Mid Z projection is shown. (b-c) RT-PCR analysis shows alternative splicing pattern of *Clcn1* exon 7A, *Nfix* exon 7 and *Serca1* exon 22 in NSG-HSA^{LR} muscles injected with satellite cells or PBS (b), and respective quantification (c). Data are shown as mean + SEM. $N = 3$ transplanted muscles, one per mouse.

with proper alternative splicing, leading to fully functional proteins that would dilute the endogenous ones, thus contributing to phenotype recovery. Here we show this is not the case since upon successful engraftment of hiPS cell-derived myogenic progenitors in immunodeficient DM1 mice, we found that donor-derived myonuclei are positive for RNA foci, resulting in disrupted alternative splicing of

donor-derived transcripts. This finding was consistent regardless of the myogenic cell type transplanted (i. e. human skeletal myoblasts, mouse satellite cells, and mES-derived myogenic progenitors) or the injury method used prior to transplantation [48].

Our results suggest a dynamic behavior of the RNAs containing CUG expansions, by which these are able to migrate to other nuclei within a muscle fiber and form RNA foci. Notably, we did not reliably detect RNA foci in the cytoplasm of DM1 mouse myofibers, which supports the hypothesis that toxic RNAs migrate from the nucleus as complexes less structured than foci, or alternatively, as single molecules that could not be detected by the resolution of RNA-FISH. Although DM1 RNA foci have been widely reported to be retained within the nucleus, there has been limited literature aimed at understanding foci molecular dynamics [50–56]. Of note, RNA foci have also been observed in the cytoplasm of different cell types, such as patient-derived DM1 myoblasts and fibroblasts [54,55], but this has been mainly attributed to cell division causing the aggregates to remain outside the nucleus after nuclear membrane disassembly, a process that would not occur in non-dividing cells, such as myotubes. Nonetheless, a potential mechanism in which toxic RNA molecules are actively exported has not been completely ruled out [55,57]. For instance, it has been shown that the RNA-binding protein Staufen1 (STAU1) interacts with and promotes the nuclear export of DMPK 3'UTR transcripts containing expanded CUG triplets [50]. This becomes relevant as in the same study, the authors also showed that STAU1 is increased in skeletal muscle tissue of DM1 patients and DM1 mouse models, such as HSA^{LR} [50]. Notably, STAU1 was not found to co-localize with foci, in line with the hypothesis that the toxic RNA export may occur as individual molecules not detectable by RNA-FISH. This premise is corroborated by a study showing that unwinding of CUG-repeats secondary structures by the DEAD-box RNA helicase DDX6 also increases the abundance of cytoplasmic mutant transcripts [54]. Moreover, it has been shown that an individual CUG^{n}-containing mRNA is sufficient to interact with MBNL1, a protein known to undergo a dynamic nucleus-cytoplasmic transport, thus enabling a possible nuclear export mechanism by means of single molecules of MBNL1 carrying single molecules of RNA [51,58,59]. Interestingly, a previous study documented that in *in vitro*-differentiated heterokaryons consisting of human DM1 myonuclei and control mouse myonuclei, alternative splicing of mouse transcripts is affected by human *DMPK* mutant mRNAs [60]. Of note, no foci were observed in mouse nuclei, despite detection of mouse splicing alterations. This could be related to the time of heterokaryons formation, i. e. *in vitro* hybrid myotubes were analyzed five days after differentiation while our *in vivo* transplantation experiments were analyzed 30 days post-transplantation. This finding goes in line with our *in vivo* observations suggesting that *DMPK* mutant transcripts exit the nucleus in which they were synthesized to cause toxicity in other myonuclei within the syncytium.

Similar to other muscular dystrophies, mouse models of DM1 that reliably resemble the muscle phenotype and course of the disease while harboring the human mutation are lacking [61,62]. In spite of this limitation, the HSA^{LR} mouse model has been successfully used in the investigation of the i) mechanisms underlining DM1and the ii) testing of therapeutic approaches, such as the use of antisense oligonucleotides [63]. For the purposes of this study, it is essential to consider that the HSA^{LR} mouse model expresses toxic RNA at higher levels than in the context of human DM1, which could lead to saturation and re-aggregation of RNA foci among myonuclei. This possibility remains to be tested by performing cell transplantation studies using DM1 mouse models expressing the CTG expansions in the context of the *DMPK* gene [13]. Nonetheless, our results provide the first precedent of a potential outcome that would need to be considered for DM1 cell therapy. Moreover, from the molecular point of view, we show evidence not only of toxic RNA export to the cytoplasm, but also of the ability of this RNA to be imported into other nuclei within the same muscle fiber and having pathological consequences. This is particularly relevant in the design of a therapy for DM1 since alternative approaches currently under investigation, such as genome editing, may encounter similar challenges. It is possible that within a myofiber, toxic RNA from non-gene edited myonuclei may be toxic to the successfully corrected ones.

Although mechanistic studies are still required to decipher the dynamic behavior of DM1 toxic RNA in myofibers, our cell transplantation results shed new light on toxic RNA nucleus/cytoplasm transport and opens a new perspective on DM1 molecular pathogenesis. Furthermore, our findings suggest a potential communication among nuclei within a myofiber *via* RNA export/import, a possibility that, to our knowledge, has not been foreseen.

Supplementary data to this article can be found online at https://doi.org/10.1016/j.ebiom.2019.08.031.

Funding sources

This project was supported by funds from the LaBonte/Shawn family and NIH grants R01 AR055299 and AR071439 (R.C.R.P.). R.M-G. was funded by CONACyT-Mexico (#394378). Funding sources were not involved in the study design, collection, analysis or interpretation of data, or decision to submit the work for publication.

Author contributions

R.M-G. designed and performed experiments, analyzed the data and wrote the manuscript; K.A. and S.S. designed and performed experiments, and analyzed the data, A.Y. performed experiments and analyzed the data. R.C.R.P. supervised the study, contributed with experimental design and interpretation of the data, and wrote the manuscript.

Declaration of Competing Interest

The authors declare no competing financial interests.

Acknowledgements

We thank Charles Thornton (University of Rochester) for the HSA^{LR} mice, Mark Sanders for guidance with confocal imaging analysis, and Michael Kyba for critical reading the manuscript.

References

[1] Harper PS. Myotonic dystrophy . 3rd ed.London: Harcourt Publishers Ltd; 2001.
[2] Norwood FL, Harling C, Chinnery PF, Eagle M, Bushby K, Straub V. Prevalence of genetic muscle disease in Northern England: in-depth analysis of a muscle clinic population. Brain 2009;132:3175–86 Pt 11.
[3] Arsenault ME, Prevost C, Lescault A, Laberge C, Puymirat J, Mathieu J. Clinical characteristics of myotonic dystrophy type 1 patients with small CTG expansions. Neurology 2006;66(8):1248–50.
[4] Bouchard JP, Cossette L, Bassez G, Puymirat J. Natural history of skeletal muscle involvement in myotonic dystrophy type 1: a retrospective study in 204 cases. J Neurol 2015;262(2):285–93.
[5] Mahadevan M, Tsilfidis C, Sabourin L, Shutler G, Amemiya C, Jansen G, et al. Myotonic dystrophy mutation: an unstable CTG repeat in the 3′ untranslated region of the gene. Science 1992;255(5049):1253–5.
[6] Jasinska A, Michlewski G, de Mezer M, Sobczak K, Kozlowski P, Napierala M, et al. Structures of trinucleotide repeats in human transcripts and their functional implications. Nucleic Acids Res 2003;31(19):5463–8.
[7] Napierala M, Krzyzosiak WJ. CUG repeats present in myotonin kinase RNA form metastable "slippery" hairpins. J Biol Chem 1997;272(49):31079–85.
[8] Taneja KL, McCurrach M, Schalling M, Housman D, Singer RH. Foci of trinucleotide repeat transcripts in nuclei of myotonic dystrophy cells and tissues. J Cell Biol 1995;128(6):995–1002.
[9] Tian B, White RJ, Xia T, Welle S, Turner DH, Mathews MB, et al. Expanded CUG repeat RNAs form hairpins that activate the double-stranded RNA-dependent protein kinase PKR. Rna 2000;6(1):79–87.
[10] Meola G, Cardani R. Myotonic dystrophies: an update on clinical aspects, genetic, pathology, and molecular pathomechanisms. Biochim Biophys Acta 2015;1852(4):594–606.
[11] Tang ZZ, Yarotskyy V, Wei L, Sobczak K, Nakamori M, Eichinger K, et al. Muscle weakness in myotonic dystrophy associated with misregulated splicing and altered gating of Ca(V)1.1 calcium channel. Hum Mol Genet 2012;21(6):1312–24.

[12] Kanadia RN, Johnstone KA, Mankodi A, Lungu C, Thornton CA, Esson D, et al. A muscleblind knockout model for myotonic dystrophy. Science 2003;302(5652):1978–80.
[13] Gomes-Pereira M, Foiry L, Nicole A, Huguet A, Junien C, Munnich A, et al. CTG trinucleotide repeat "big jumps": large expansions, small mice. PLoS Genet 2007;3(4):e52.
[14] Mankodi A, Logigian E, Callahan L, McClain C, White R, Henderson D, et al. Myotonic dystrophy in transgenic mice expressing an expanded CUG repeat. Science 2000;289(5485):1769–73.
[15] Orengo JP, Chambon P, Metzger D, Mosier DR, Snipes GJ, Cooper TA. Expanded CTG repeats within the DMPK 3' UTR causes severe skeletal muscle wasting in an inducible mouse model for myotonic dystrophy. Proc Natl Acad Sci USA 2008;105(7):2646–51.
[16] Mulders SA, van den Broek WJ, Wheeler TM, Croes HJ, van Kuik-Romeijn P, de Kimpe SJ, et al. Triplet-repeat oligonucleotide-mediated reversal of RNA toxicity in myotonic dystrophy. Proc Natl Acad Sci USA 2009;106(33):13915–20.
[17] Pandey SK, Wheeler TM, Justice SL, Kim A, Younis HS, Gattis D, et al. Identification and characterization of modified antisense oligonucleotides targeting DMPK in mice and nonhuman primates for the treatment of myotonic dystrophy type 1. J Pharmacol Exp Ther 2015;355(2):329–40.
[18] Wheeler TM, Leger AJ, Pandey SK, MacLeod AR, Nakamori M, Cheng SH, et al. Targeting nuclear RNA for in vivo correction of myotonic dystrophy. Nature 2012;488(7409):111–5.
[19] Negroni E, Gidaro T, Bigot A, Butler-Browne GS, Mouly V, Trollet C. Invited review: stem cells and muscle diseases: advances in cell therapy strategies. Neuropathol Appl Neurobiol 2015;41(3):270–87.
[20] Quattrocelli M, Cassano M, Crippa S, Perini I, Sampaolesi M. Cell therapy strategies and improvements for muscular dystrophy. Cell Death Differ 2010;17(8):1222–9.
[21] Tedesco FS, Gerli MF, Perani L, Benedetti S, Ungaro F, Cassano M, et al. Transplantation of genetically corrected human iPSC-derived progenitors in mice with limb-girdle muscular dystrophy. Sci Transl Med 2012;4(140):140ra89.
[22] Sampaolesi M, Blot S, D'Antona G, Granger N, Tonlorenzi R, Innocenzi A, et al. Mesoangioblast stem cells ameliorate muscle function in dystrophic dogs. Nature 2006;444(7119):574–9.
[23] Cerletti M, Jurga S, Witczak CA, Hirshman MF, Shadrach JL, Goodyear LJ, et al. Highly efficient, functional engraftment of skeletal muscle stem cells in dystrophic muscles. Cell 2008;134(1):37–47.
[24] Arpke RW, Darabi R, Mader TL, Zhang Y, Toyama A, Lonetree CL, et al. A new immuno-, dystrophin-deficient model, the NSG-mdx(4Cv) mouse, provides evidence for functional improvement following allogeneic satellite cell transplantation. Stem Cells 2013;31(8):1611–20.
[25] Partridge TA, Morgan JE, Coulton GR, Hoffman EP, Kunkel LM. Conversion of mdx myofibres from dystrophin-negative to -positive by injection of normal myoblasts. Nature 1989;337(6203):176–9.
[26] Darabi R, Arpke RW, Irion S, Dimos JT, Grskovic M, Kyba M, et al. Human ES- and iPS-derived myogenic progenitors restore DYSTROPHIN and improve contractility upon transplantation in dystrophic mice. Cell Stem Cell 2012;10(5):610–9.
[27] Coughlan AM, Harmon C, Whelan S, O'Brien EC, O'Reilly VP, Crotty P, et al. Myeloid engraftment in humanized mice: impact of granulocyte-colony stimulating factor treatment and transgenic mouse strain. Stem Cells Dev 2016;25(7):530–41.
[28] Shultz LD, Lyons BL, Burzenski LM, Gott B, Chen X, Chaleff S, et al. Human lymphoid and myeloid cell development in NOD/LtSz-scid IL2R gamma null mice engrafted with mobilized human hemopoietic stem cells. J Immunol 2005;174(10):6477–89.
[29] Hadjantonakis AK, Papaioannou VE. Dynamic in vivo imaging and cell tracking using a histone fluorescent protein fusion in mice. BMC Biotechnol 2004;4:33.
[30] DiFranco M, Yu C, Quinonez M, Vergara JL. Age-dependent chloride channel expression in skeletal muscle fibres of normal and HSA(LR) myotonic mice. J Physiol 2013;591(5):1347–71.
[31] Magli A, Perlingeiro RRC. Myogenic progenitor specification from pluripotent stem cells. Semin Cell Dev Biol 2017;72:87–98.
[32] Iacovino M, Bosnakovski D, Fey H, Rux D, Bajwa G, Mahen E, et al. Inducible cassette exchange: a rapid and efficient system enabling conditional gene expression in embryonic stem and primary cells. Stem Cells 2011;29(10):1580–8.
[33] Magli A, Incitti T, Perlingeiro RC. Myogenic progenitors from mouse pluripotent stem cells for muscle regeneration. Methods Mol Biol 2016;1460:191–208.
[34] Incitti T, Magli A, Darabi R, Yuan C, Lin K, Arpke RW, et al. Pluripotent stem cell-derived myogenic progenitors remodel their molecular signature upon in vivo engraftment. Proc Natl Acad Sci USA 2019;116(10):4346–51.
[35] Arpke RW, Kyba M. Flow cytometry and transplantation-based quantitative assays for satellite cell self-renewal and differentiation. Methods Mol Biol 2016;1460:163–79.
[36] Darabi R, Santos FN, Filareto A, Pan W, Koene R, Rudnicki MA, et al. Assessment of the myogenic stem cell compartment following transplantation of Pax3/Pax7-induced embryonic stem cell-derived progenitors. Stem Cells 2011;29(5):777–90.
[37] Tierney MT, Sacco A. Inducing and evaluating skeletal muscle injury by notexin and barium chloride. Methods Mol Biol 2016;1460:53–60.
[38] Le G, Lowe DA, Kyba M. Freeze injury of the tibialis anterior muscle. Methods Mol Biol 2016;1460:33–41.
[39] Hall LL, Carone DM, Gomez AV, Kolpa HJ, Byron M, Mehta N, et al. Stable C0T-1 repeat RNA is abundant and is associated with euchromatic interphase chromosomes. Cell 2014;156(5):907–19.
[40] Han KD, Mafi A, Johnson MD, Cohen M, Gbulie UB, Baker SB. Application of fluorescent in situ hybridization in the mouse xenograft model of human fat grafting. Aesthet Surg J 2012;32(6):745–50.
[41] Chen G, Masuda A, Konishi H, Ohkawara B, Ito M, Kinoshita M, et al. Phenylbutazone induces expression of MBNL1 and suppresses formation of MBNL1-CUG RNA foci in a mouse model of myotonic dystrophy. Sci Rep 2016;6:25317.
[42] Warf MB, Nakamori M, Matthys CM, Thornton CA, Berglund JA. Pentamidine reverses the splicing defects associated with myotonic dystrophy. Proc Natl Acad Sci USA 2009;106(44):18551–6.
[43] Hino S, Kondo S, Sekiya H, Saito A, Kanemoto S, Murakami T, et al. Molecular mechanisms responsible for aberrant splicing of SERCA1 in myotonic dystrophy type 1. Hum Mol Genet 2007;16(23):2834–43.
[44] Yamashita Y, Matsuura T, Kurosaki T, Amakusa Y, Kinoshita M, Ibi T, et al. LDB3 splicing abnormalities are specific to skeletal muscles of patients with myotonic dystrophy type 1 and alter its PKC binding affinity. Neurobiol Dis 2014;69:200–5.
[45] Bosma GC, Custer RP, Bosma MJ. A severe combined immunodeficiency mutation in the mouse. Nature 1983;301(5900):527–30.
[46] Cao X, Shores EW, Hu-Li J, Anver MR, Kelsall BL, Russell SM, et al. Defective lymphoid development in mice lacking expression of the common cytokine receptor gamma chain. Immunity 1995;2(3):223–38.
[47] Ishikawa F, Yasukawa M, Lyons B, Yoshida S, Miyamoto T, Yoshimoto G, et al. Development of functional human blood and immune systems in NOD/SCID/IL2 receptor {gamma} chain(null) mice. Blood 2005;106(5):1565–73.
[48] Mondragon-Gonzalez R, Perlingeiro RCR. Recapitulating muscle disease phenotypes with myotonic dystrophy 1 iPS cells: a tool for disease modeling and drug discovery. Dis Model Mech 2018;11(7) (dmm034728).
[49] Kimura T, Nakamori M, Lueck JD, Pouliquin P, Aoike F, Fujimura H, et al. Altered mRNA splicing of the skeletal muscle ryanodine receptor and sarcoplasmic/endoplasmic reticulum Ca2+-ATPase in myotonic dystrophy type 1. Hum Mol Genet 2005;14(15):2189–200.
[50] Ravel-Chapuis A, Belanger G, Yadava RS, Mahadevan MS, DesGroseillers L, Cote J, et al. The RNA-binding protein Staufen1 is increased in DM1 skeletal muscle and promotes alternative pre-mRNA splicing. J Cell Biol 2012;196(6):699–712.
[51] Querido E, Gallardo F, Beaudoin M, Menard C, Chartrand P. Stochastic and reversible aggregation of mRNA with expanded CUG-triplet repeats. J Cell Sci 2011;124(10):1703–14.
[52] Kim DH, Langlois MA, Lee KB, Riggs AD, Puymirat J, Rossi JJ. HnRNP H inhibits nuclear export of mRNA containing expanded CUG repeats and a distal branch point sequence. Nucleic Acids Res 2005;33(12):3866–74.
[53] Davis BM, McCurrach ME, Taneja KL, Singer RH, Housman DE. Expansion of a CUG trinucleotide repeat in the 3′ untranslated region of myotonic dystrophy protein kinase transcripts results in nuclear retention of transcripts. Proc Natl Acad Sci USA 1997;94(14):7388–93.
[54] Pettersson OJ, Aagaard L, Andrejeva D, Thomsen R, Jensen TG, Damgaard CK. DDX6 regulates sequestered nuclear CUG-expanded DMPK-mRNA in dystrophia myotonica type 1. Nucleic Acids Res 2014;42(11):7186–200.
[55] Dansithong W, Wolf CM, Sarkar P, Paul S, Chiang A, Holt I, et al. Cytoplasmic CUG RNA foci are insufficient to elicit key DM1 features. PloS One 2008;3(12):e3968.
[56] Jain A, Vale RD. RNA phase transitions in repeat expansion disorders. Nature 2017;546(7657):243–7.
[57] Pettersson OJ, Aagaard L, Jensen TG, Damgaard CK. Molecular mechanisms in DM1 - a focus on foci. Nucleic Acids Res 2015;43(4):2433–41.
[58] Coleman SM, Prescott AR, Sleeman JE. Transcriptionally correlated subcellular dynamics of MBNL1 during lens development and their implication for the molecular pathology of myotonic dystrophy type 1. Biochem J 2014;458(2):267–80.
[59] Wang PY, Chang KT, Lin YM, Kuo TY, Wang GS. Ubiquitination of MBNL1 is required for its cytoplasmic localization and function in promoting neurite outgrowth. Cell Rep 2018;22(9):2294–306.
[60] Ferreboeuf M, Mariot V, Furling D, Butler-Browne G, Mouly V, Dumonceaux J. Nuclear protein spreading: implication for pathophysiology of neuromuscular diseases. Hum Mol Genet 2014;23(15):4125–33.
[61] Gomes-Pereira M, Cooper TA, Gourdon G. Myotonic dystrophy mouse models: towards rational therapy development. Trends Mol Med 2011;17(9):506–17.
[62] Ng R, Banks GB, Hall JK, Muir LA, Ramos JN, Wicki J, et al. Animal models of muscular dystrophy. Prog Mol Biol Transl Sci 2012;105:83–111.
[63] Wheeler TM, Sobczak K, Lueck JD, Osborne RJ, Lin X, Dirksen RT, et al. Reversal of RNA dominance by displacement of protein sequestered on triplet repeat RNA. Science 2009;325(5938):336–9.